Heliyon

Received:
31 August 2017
Revised:
29 December 2017
Accepted:
8 January 2018

Cite as: Jorge A. Avila, Roseanna M. Zanca, Denis Shor, Nicholas Paleologos, Amber A. Alliger, Maria E. Figueiredo-Pereira, Peter A. Serrano. Chronic voluntary oral methamphetamine induces deficits in spatial learning and hippocampal protein kinase Mzeta with enhanced astrogliosis and cyclooxygenase-2 levels. Heliyon 4 (2018) e00509. doi: 10.1016/j.heliyon.2018.e00509

Chronic voluntary oral methamphetamine induces deficits in spatial learning and hippocampal protein kinase Mzeta with enhanced astrogliosis and cyclooxygenase-2 levels

Jorge A. Avila [a,c], **Roseanna M. Zanca** [a,c], **Denis Shor** [a], **Nicholas Paleologos** [a,1], **Amber A. Alliger** [a], **Maria E. Figueiredo-Pereira** [b,c], **Peter A. Serrano** [a,c,*]

[a] *Department of Psychology, Hunter College, City University of New York, New York, NY, USA*

[b] *Department of Biological Sciences, Hunter College, City University of New York, New York, NY, USA*

[c] *The Graduate Center of CUNY, New York, NY, USA*

* Corresponding author.

E-mail address: serrano@genectr.hunter.cuny.edu (P.A. Serrano).

[1] Present address: Department of Biology, University of Pennsylvania, Philadelphia, PA, USA.

Abstract

Methamphetamine (MA) is an addictive drug with neurotoxic effects on the brain producing cognitive impairment and increasing the risk for neurodegenerative disease. Research has focused largely on examining the neurochemical and behavioral deficits induced by injecting relatively high doses of MA [30 mg/kg of body weight (bw)] identifying the upper limits of MA-induced neurotoxicity. Accordingly, we have developed an appetitive mouse model of voluntary oral MA administration (VOMA) based on the consumption of a palatable sweetened oatmeal mash containing a known amount of MA. This VOMA model is useful for determining the lower limits necessary to produce neurotoxicity in the short-term and long-term as it progresses over time. We show that mice consumed on average

http://dx.doi.org/10.1016/j.heliyon.2018.e00509

1.743 mg/kg bw/hour during 3 hours, and an average of 5.23 mg/kg bw/day over 28 consecutive days on a VOMA schedule. Since this consumption rate is much lower than the neurotoxic doses typically injected, we assessed the effects of long-term chronic VOMA on both spatial memory performance and on the levels of neurotoxicity in the hippocampus. Following 28 days of VOMA, mice exhibited a significant deficit in short-term spatial working memory and spatial reference learning on the radial 8-arm maze (RAM) compared to controls. This was accompanied by a significant decrease in memory markers protein kinase Mzeta (PKMζ), calcium impermeable AMPA receptor subunit GluA2, and the post-synaptic density 95 (PSD-95) protein in the hippocampus. Compared to controls, the VOMA paradigm also induced decreases in hippocampal levels of dopamine transporter (DAT) and tyrosine hydroxylase (TH), as well as increases in dopamine 1 receptor (D1R), glial fibrillary acidic protein (GFAP) and cyclooxygenase-2 (COX-2), with a decrease in prostaglandins E2 (PGE2) and D2 (PGD2). These results demonstrate that chronic VOMA reaching 146 mg/kg bw/28d induces significant hippocampal neurotoxicity. Future studies will evaluate the progression of this neurotoxic state.

Keywords: Neuroscience

1. Introduction

Methamphetamine (MA) abuse is a costly and detrimental health risk in the U.S. and abroad. In the U.S., the number of individuals who reported abusing MA in 2012 was approximately 1.2 million people (4.7 percent of the population) (NIDA, 2013). Amphetamine-type stimulants (ATS) now rank second only to cannabis as the most common illicit drugs used worldwide, representing approximately 34 million users (UN, 2008). North America continues to be a significant market for ATS, particularly amphetamine and methamphetamine (UN, 2011). Based on these statistics, it becomes increasingly important that we understand the risk factors associated with MA addiction, and develop new animal models to better address treatment outcomes for addicts. It is well known that MA abusers show a long-lasting reduction in dopamine terminals and transporters, both of which increase the risk for Parkinson's Disease (McCann et al., 2008; Volkow et al., 2015). Chronic MA abuse also results in neurodegeneration of frontal cortex, midbrain regions and hippocampus, which are all associated with memory deficits (Thompson et al., 2004). Additionally, an increase in markers of neuroinflammation, including activated microglia was reported in MA abusers (Sekine et al., 2008). Several animal studies have recapitulated many of these neurochemical and behavioral characteristics associated with MA abuse [reviewed in (Cadet and Krasnova, 2009)]. Many animal studies show that neurotoxic or binge-dosing regiments of MA produce rapid increases in microglia (LaVoie et al., 2004) and glial fibrillary acidic protein (GFAP) levels within the striatum and hippocampus

http://dx.doi.org/10.1016/j.heliyon.2018.e00509

(Goncalves et al., 2010; Narita et al., 2005; Simoes et al., 2007) shortly after administration.

While there are many MA paradigms for rodents currently used, what is needed is a model that capitalizes on the voluntary MA consumption without the need for conditioning to administer the drug or surgery that can restrict the types of behavioral assessments used. Here we provide data on a voluntary oral methamphetamine administration (VOMA) model useful for determining the progressive nature of voluntary abuse-associated neurotoxicity in a rodent model. Our goal was to assess the effectiveness of this VOMA model in producing hippocampal-dependent memory and learning deficits, as well as MA-associated neurochemical changes. To evaluate cognitive behavior we used the radial arm maze (RAM), which is a hippocampal-dependent task (Jarrard, 1978; Olton and Papas, 1979) used to assess both long-term reference and short-term working memories (Braren et al., 2014).

Following behavioral assessments, we quantified changes in (1) dopamine-related markers involving tyrosine hydroxylase (TH), dopamine transporter (DAT), and the Dopamine 1 receptor (D1R); (2) glutamate receptor alpha-amino-3-hydroxy-5-methylisoxazole-4-propionate (AMPA) GluA2 subunit; (3) atypical protein kinase C iota/lambda (PKCι/λ), protein kinase Mzeta (PKMζ) and the post-synaptic density 95 (PSD-95) protein; and (4) markers of inflammation involving astrogliosis measured by GFAP, cycloxygenase-2 (COX-2), and prostaglandins (PG) E2, D2 and J2. We focused on these molecular markers since MA selectively damages DA terminals and produces excitotoxicity effects involving AMPA receptors (Bowers et al., 2010; Kalivas and Volkow, 2011) in addition to elevated levels of inflammation (Simoes et al., 2007). Astrogliosis is associated with MA neurotoxicity and several other toxic insults in the brain (O'Callaghan and Sriram, 2005). Finally, as a synaptic plasticity and memory marker, we focused on the atypical kinase PKMζ that is important for spatial learning and long-term memory (Sebastian et al., 2013b; Serrano et al., 2008), and which is increased concomitantly with improved memory (Sebastian et al., 2013c) across several memory paradigms [reviewed in (Sacktor, 2011)].

Our results show that 28d on VOMA produces significant deficits in hippocampal-dependent short-term working and long-term reference learning on the RAM. These behavioral deficits were associated with decreases in PKMζ, GluA2 and PSD-95. VOMA also produced decreases in DAT and TH, with a concomitant increase in D1R levels. Both GFAP and COX-2 increased, with decreases in PGE2 and PGD2. Thus, these results highlight the accumulating negative effects of chronic VOMA in addition to its usefulness in characterizing the progression of the MA-induced neurotoxicity.

http://dx.doi.org/10.1016/j.heliyon.2018.e00509

2. Material and methods

2.1. Mice

All experimental conditions, housing, and drug administration procedures were reviewed and approved by the Institutional Animal Care and Use Committee (IACUC) of Hunter College. Male C57BL/6 mice from Taconic Farms (Germantown, NY) were purchased at 8 weeks of age. Mice were randomly assigned to 2 treatment conditions: MA (n = 5) and Control (n = 5). We have used similar sample sizes to evaluate behavioral performance and protein expression as previously reported (Braren et al., 2014; Sebastian et al., 2013a; 2013c). Mice were housed individually to control for social effects of group housing (Weber et al., 2017) that could affect the voluntary consumption of methamphetamine in our model. Mice were kept on a 12/12 h light/dark cycle at the Hunter College animal facility for one week prior to beginning any behavioral assessments with food and water *ad libitum* prior to behavioral shaping. All housing conditions conform to the Hunter College guidelines outlined by the IACUC.

2.2. Methamphetamine Treatment

We used a new voluntary oral methamphetamine administration (VOMA) model over 28 consecutive days (experimental days 5–32). A sweetened oatmeal flake (Maypo, Homestat Farm, Dublin, OH) was moistened with 8–10 μl of either MA (2.5 mg/ml) or water. This produces a palatable sweetened oatmeal flake that contains 1 mg MA/kg of body weight (bw) per serving (adjusted to mice ranging in weight between 20–25 g). During MA administration, all mice were transferred to individual mouse cages that were lined with absorbent paper. Each cage was designated to a specific mouse throughout the experiment to ensure context specificity. Cages were wiped clean and lined with fresh paper after each use. All mice remained in their paper-lined cage for 30 min prior to treatment. During a 3 hour (hr) period, from 13:00 h to 16:00 h, mice were presented with individual MA or water moistened oatmeal flakes. A new presentation was delivered in a clean petri dish every 15 min. For each mouse, the number of consumed flakes during the 3 hr period was noted. Directly after VOMA, all mice were fed 4 g of mouse chow daily at 18:00 h. This feeding schedule ensured that mice would be willing to consume oatmeal flakes during the VOMA treatment time-window, for 28 consecutive days. This feeding schedule also circumvented the significant circadian effects reported on VOMA administration (Keith et al., 2013), without disrupting weight gain throughout the duration of the experiment.

2.3. Radial 8-arm maze shaping

The radial 8-arm maze (RAM) was used to assess both working memory and spatial learning performance. The maze consists of a center platform (15.24 cm

http://dx.doi.org/10.1016/j.heliyon.2018.e00509

diameter) with 8 equivalently sized arms radiating outward. Each arm is 38 cm in length, 6.35 cm wide and has a submerged food cup (2.0 cm diameter) at the end of each arm. Maypo was mixed in water to make a wet mash used as a food reward (0.02 g portions), as previously described for mice (Braren et al., 2014) and rats (Serrano et al., 2008). Prior to working memory assessments, all animals were shaped on the RAM during days 1–2 of the study. Mice were food restricted to 85% of free feeding weight before being placed on the RAM for 10 min to acclimate to the maze and room cues. 1 hr later, all mice were given a second trial with sweetened oatmeal in the food cups. After 1 day of shaping (2 trials per day), mice were eating the food rewards and finding all 8 baits within a 15 min maximum latency.

2.4. Working memory assessment

The working memory assessment (WMA) occurred during experimental day 37. Mice were tested for 1 day (3 consecutive trials). Each trial started with all food cups baited. To begin each trial, mice were confined for 30 s to the center platform with a plastic cylinder. Between trials mice were confined to the center platform while the arms were re-baited and the maze cleaned. The sequence of arms entered to retrieve the food rewards was recorded. Mice were allowed to collect baits from up to 3 sequential arms in any direction around the radial arm maze. Under rare instances when a mouse adopted a chaining strategy by entering consecutive arms in one direction around the maze, the 4th sequential arm was blocked to disrupt this non-spatial strategy (Braren et al., 2014). Errors were recorded as re-entries into arms where the food reward had already been collected. Working memory was assessed by a % correct score for each trial, which was calculated by the number of total arm entries required to collect all 8 food rewards divided by 8 (the total number of rewards collected). All mice remained on the maze until all 8 baits were collected. Maximum latency for each trial was set at 15 min.

2.5. Spatial learning/cognitive flexibility assessment

During experimental days 40–49, all mice were trained on a reference and working memory version of the RAM as previously reported (Braren et al., 2014). This paradigm had 4 baited and 4 un-baited arms in a pattern that was specific to each animal and remained constant throughout the experiment. Mice were given 6 consecutive trials per day for 10 days (60 trials total). Between trials mice were confined to the center platform while the arms were re-baited and the maze cleaned. The sequence of arm entries was recorded. A reference memory error reflected an entry into an arm that was never baited, while working memory errors reflected re-entries into an arm where the bait had already been collected. Mice were only allowed to enter up to 3 sequential arms to prevent the non-hippocampal dependent chaining strategy. This version of the RAM required mice to learn room

http://dx.doi.org/10.1016/j.heliyon.2018.e00509

cues associated with the baited and un-baited arm sequence. The training room and room cues were identical to that used for the WMA. 24 hrs after the last RAM trial, all mice were given one reminder trial on the maze 1 hr prior to tissue retrieval. Hippocampi from each mouse were removed, snap frozen and stored at −80 °C until processed further.

2.6. Preparation of tissue fractions

Hippocampi were micro dissected and fractionated into cytosolic and synaptic fractions as previously reported (Braren et al., 2014). Briefly, tissues were thawed and homogenized in a TEE (Tris 50 mM; EDTA 1 mM; EGTA 1 mM) buffer containing a Sigma Fast, protease inhibitor cocktail (Sigma Aldrich) diluted to contain AEBSF (2 mM), Phosphoramidon (1 mM), Bestatin (130 mM), E-64 (14 mM), Leupeptin (1 mM), Aprotinin (0.2 mM), and PepstatinA (10 mM). Tissues were homogenized in 200 μl of the TEE-homogenization buffer using 20 pumps with a motorized pestle. Homogenates were transferred to Eppendorf tubes and centrifuged at 3000 x g (5 min at 4 °C), to remove un-homogenized tissue. The resulting supernatant was centrifuged at 100,000 g for 30 min. After ultracentrifugation, the supernatant was collected and stored as the cytosolic fraction. The remaining pellet was re-suspended in 100 μl of homogenizing TEE buffer containing 0.001% Triton X–100, incubated on ice for 1 hr and then centrifuged at 100,000 g for 1 hr at 4 °C. The resulting supernatant was stored at the plasma-membrane fraction. The resulting pellet was re-suspended in 50 μl of TEE buffer and stored as the synaptic fraction (Nogues et al., 1994). The Pierce bicinchoninic acid assay (BCA; Thermo Scientific, Rockford, IL, USA) was used to determine protein concentration for each sample. Samples were reduced with 4x Laemmli sample buffer equivalent to 25% of the total volume of the sample and then boiled and stored frozen at −80 °C.

2.7. Immunoblots

Samples (20 μg) were loaded on to a Tris/Glycine 4–20% mini gel to resolve GAPDH (37 kDa), α-Tubulin (55 kDa), PKMζ (55 kDa), PKCι/λ (68 kDa), GluA2 (98 kDa), PSD-95 (95 kDa), COX-2 (72 kDa), GFAP (53 kDa), TH (60 kDa), D1 (49 kDa) and DAT (69 kDa). Every gel contained 4 lanes loaded with the same control sample designated as all brain sample (ABS). ABS was used to standardize protein signals between gels. Gels were transferred to nitrocellulose membranes in the IBlot® Dry Blotting System (Life Technologies; Carlsbad, CA, USA) for 7 min. Nitrocellulose membranes were then incubated in blocking solution containing 5% sucrose in Tris Buffered Saline with Tween-20 (TBST; 0.1% Tween-20 in TBS) for 30 min at room temperature. Samples were incubated overnight with the following primary antibodies: GluA2 (1:2000; Chemicon, Temecula, CA, USA), PKMζ/PKCι/λ (1:2000; Santa Cruz Biotechnology, Santa

http://dx.doi.org/10.1016/j.heliyon.2018.e00509

Cruz, CA, USA), GAPDH (1:2000; Abcam Inc., Cambridge, MA, USA), PSD-95 (1:1000; Cell Signaling Technology, Danvers, MA, USA), COX-2 (1:1000; Santa Cruz Biotechnology, Santa Cruz, CA, USA), GFAP (1:5000; Abcam Inc., Cambridge, MA, USA), TH (1:2000; ab152, Millipore, Billerica, MA, USA), D1 (1:2000; Abcam Inc., Cambridge, MA, USA), DAT (1:1000; EMD Millipore, Temecula, CA, USA) and α-Tubulin (1:2000; Calbiochem, San Diego, CA, USA). Membranes were washed in TBST for 20 min and probed with Horseradish Peroxidase (HRP) conjugated secondary antibodies: Goat Anti-Mouse IgG (H + L)-HRP Conjugate #1706516 (BioRad); Goat Anti-Rabbit IgG (H + L)-HRP Conjugate #1706515 (BioRad); Rabbit Anti-Goat IgG H&L (HRP) (ab6741-Abcam). Membranes were incubated with Enhanced Chemiluminescence (ECL) substrate and exposed on CL-X Posure Film (Thermo Scientific; Rockford, IL, USA). Films were scanned, and then densitometry was performed with NIH ImageJ (Vierck et al., 2000).

2.8. Preparation of samples for prostaglandin quantification

For prostaglandin quantification, pre-weighed hippocampal tissues were homogenized in 0.9 ml of phosphate buffered saline using a BeadBug microtube homogenizer. Following homogenization, a 10-mg wet weight equivalent of homogenate was removed and diluted to a final volume of 10 mg per 0.9 ml before being further diluted 1:1 with 1% formic acid. Deuterated internal standards were added (identified in italics in Table below) to the diluted homogenate and loaded on a 2 ml Biotage SLE+ cartridge. After a 5 min incubation, the cartridges were eluted twice with 6 ml of t-butlymethylether. The eluent was spiked with 20 µl of a trap solution consisting of 10% glycerol in methanol with 0.01 mg/ml butylated hydroxytoluene. The samples were dried for 45 minutes in a speed vacuum at 35 °C, the walls of the tubes were washed with 1 ml of hexane and re-dried until a small aqueous residue remained. The residue was dissolved in 50 µl of 80:20 water:acetonitrile with 0.1 mg/ml butylated hydroxytoluene and spin filtered with a 0.22 µm Millipore Ultrafree® filter. Samples were transferred to vials and 30 µl of sample were analyzed. Prostaglandin standard curves were spiked into PBS and prepared identically to the samples. Area ratios were plotted and unknowns determined using the slopes.

2.9. LC-MS/MS for prostaglandin quantification

Samples were analyzed using a 5500 Q-TRAP hybrid/triple quadrupole linear ion trap mass spectrometer (Applied Biosystems, Carlsbad, CA) with electrospray ionization (ESI) in negative mode. The mass spectrometer was interfaced to a Shimadzu (Columbia, MD) SIL-20AC XR auto-sampler followed by 2 LC-20AD XR LC pumps. The scheduled MRM transitions were monitored within a 1.5 min time-window (supplemental Table 1). Optimal instrument parameters were

http://dx.doi.org/10.1016/j.heliyon.2018.e00509

determined by direct infusion of each analyte. The gradient mobile phase was delivered at a flow rate of 0.5 ml/min, and consisted of two solvents, 0.05% acetic acid in water and acetonitrile. The analytes were resolved on a Betabasic-C18 (100 × 2 mm, 3 μm) column at 40 °C using the Shimadzu column oven. Data was acquired using Analyst 1.5.1 and analyzed using Multiquant 3.0.1(AB Sciex, Ontario, Canada).

2.10. Statistics

For behavioral analyses, a repeated measure Two-Way ANOVA was used (Prism GraphPad 7.0a Statistical Package, La Jolla, California). Post-hoc analyses used Bonferroni-corrected t-tests. Western blot and PG mass-spec analyses between MA and control treatments used independent t-tests. To characterize the generalizability of our results and support the magnitude of effects in our studies independent of sample size, effect sizes are reported. Effect sizes were calculated as generalized eta squared (η^2_G) for behavioral data and Hedge's unbiased *g* (*g*) for post-hoc analyses and molecular data, using IBM SPSS Statistics for Mac (Armonk, NY: IBM Corp.), and Microsoft Excel® as previously described (Lakens, 2013). For our studies, benchmark coefficient thresholds for large effects (Lakens, 2013) were taken into account and inflated in order to restrict significance. The thresholds for *large effect sizes* in our studies were as follows: when η^2_G was 0.2 or higher, and when *g* was 0.8 or higher. Effect sizes below these criteria were deemed moderate.

3. Results

3.1. Shaping and methamphetamine administration

The study began with shaping animals for a total of 2 days. After 4 total days of acclimation, subjects were randomly assigned to either a water/control group or MA for 28 consecutive days (days 5–32). The WMA was performed on day 37 after 5 days of forced abstinence from MA. This was followed by 10 days of cognitive flexibility assessment on the reference/working memory version of the RAM (days 40–49). Tissue was collected on day 50 (Fig. 1A). Over the 28d period mice consumed an average of 5.23 mg/kg of MA/day. Fig. 1B reflects the average weekly consumption of MA. Control mice ate every presentation of water-Maypo. Fig. 1C shows the average weekly weights for both conditions. A two-way ANOVA shows no significant difference between the groups [$F_{(1,32)} = 1.55$, $p > 0.05$; $\eta^2_G = 0.023$, non-significant effect size] indicating that the Maypo consumption, with or without MA, was not influenced by differences in body weight between conditions.

http://dx.doi.org/10.1016/j.heliyon.2018.e00509

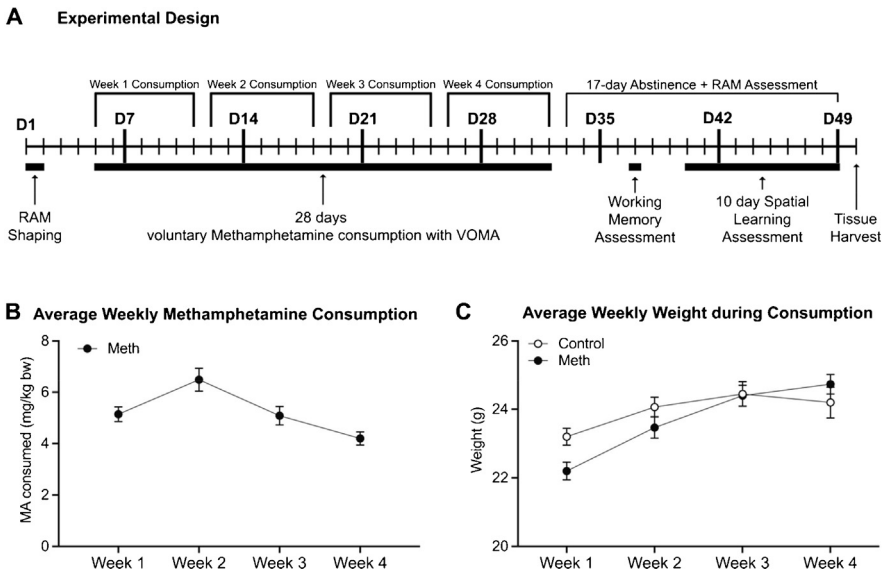

Fig. 1. Timeline for the 50d study, Average Methamphetamine (MA) Consumption and Body Weights. (A) Days 1–2: behavioral shaping on RAM. Days 5–32: VOMA for 28d. Day 37: working memory assessment. Days 40–49: cognitive flexibility assessment (spatial learning). Day 50: RAM test and tissue harvest. (B) The total amount of MA consumed over the 28 day VOMA period, grouped into 4-week averages for the Methamphetamine (Meth) group. (C) Mice were weighed during the consumption period of VOMA. No significant differences were found between the two groups when analyzed by two-way ANOVA [$F_{(1,32)} = 1.55$, $p > 0.05$; $\eta^2_G = 0.023$, non-significant effect size].

3.2. Radial- Arm-Maze working and reference memory assessments

Fig. 2A shows the % correct scores in two separate analyses to illustrate the differences in number of errors committed during a trial. Collecting the first 4 baits, when the working memory load is low, shows a much higher % correct score compared to when the working memory load is high, collecting baits 5–8. An overall 2-way ANOVA reflecting treatment condition (MA or saline) and baits (1–4 or 5–8) shows a significant effect of bait [$F_{(1,8)} = 50.67$, $p < 0.001$; $\eta^2_G = 0.76$, significant effect size]. The Bonferonni post-hoc analysis shows significant within-group differences in both control (Bonferonni corrected t-test = 3.14, $p < 0.05$; $g = 1.57$) and VOMA (Bonferonni corrected t-test = 6.93, $p < 0.001$; $g = 4.85$) mice when comparing group performances between collecting baits 1–4 and baits 5–8. Between groups, there were no significant differences between treatments for baits 1–4 (Bonferonni corrected t-test = 0.39, $p > 0.05$; $g = 0.23$) In contrast, VOMA produced a significant increase in working memory errors while collecting baits 5–8 compared to controls (Bonferroni corrected t- test = 3.41, $p < 0.01$; $g = 1.92$). Fig. 2B shows the latency to complete the working memory trials. There were no significant differences between treatment conditions for latency to complete working memory trials (Fig. 2B).

http://dx.doi.org/10.1016/j.heliyon.2018.e00509

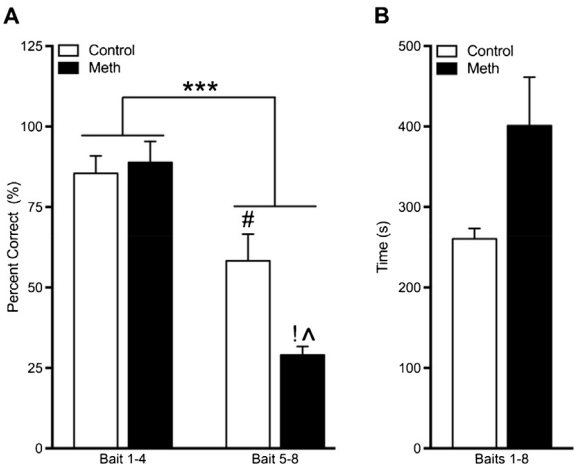

Fig. 2. VOMA impairs spatial working memory. (A) Two-way Repeated ANOVA showed an overall effect of bait group (*** $p < 0.001$). Post hoc analyses reveal that both control and Meth mice performed significantly worse to retrieve baits 5–8 compared to baits 1–4 (# indicates different from control bait 1–4, $p < 0.05$; ! indicates different from Meth bait 1–4, $p < 0.001$). Baits 5–8 reveal a significant difference between groups (^ indicates different from control in same bait condition $p < 0.01$). (B) There was no significant difference in latency to complete the trial between the groups.

Fig. 3 shows the behavioral analyses for RAM acquisition across 10 training days (experiment days 40–49 shown on graphs). An overall 2-way ANOVA for % correct scores (Fig. 3A) shows a significant interaction effect of treatment on training days [$F_{(9,72)} = 5.12$, $p < 0.01$; $\eta^2_G = 0.29$] and time [$F_{(9,72)} = 33.38$, $p < 0.01$; $\eta^2_G = 0.73$]. Post hoc tests show significant differences between treatment conditions for training day 8 (Bonferroni corrected t-test = 3.45, $p < 0.01$; $g = 1.97$) and training day 9 (Bonferroni corrected t-test = 4.28, $p < 0.01$; $g = 2.44$). To determine whether there are significant differences in asymptotic performance level between groups, we assessed % correct scores during training days 6–10 (experiment days 45–49). This analysis shows an overall effect of drug treatment [$F_{(1,8)} = 10.99$, $p < 0.05$; $\eta^2_G = 0.40$], reflecting differences in the level of peak performance. As predicted with asymptotic performance, there was no significant effect of training days. Consistent with % correct score analyses, reference memory errors shown in Fig. 3B reflect an overall significant interaction effect of treatment on training days [$F_{(9,72)} = 3.75$, $p < 0.01$; $\eta^2_G = 0.25$], and a significant effect of training days [$F_{(9,72)} = 25.00$, $p < 0.01$; $\eta^2_G = 0.69$]. During asymptotic performance (training days 6–10 experiment days 45–49), reference memory errors show an overall significant effect of treatment [$F_{(1,8)} = 13.8$, $p < 0.01$; $\eta^2_G = 0.33$]. Analysis of working memory errors (Fig. 3C) shows an overall significant effect on training [$F_{(9,72)} = 5.25$, $p < 0.01$; $\eta^2_G = 0.35$], but no significant effect between treatment conditions. During asymptotic performance (training days 6–10, experiment days 45–49), there was a significant effect of treatment [$F_{(1,8)} = 5.513$,

http://dx.doi.org/10.1016/j.heliyon.2018.e00509

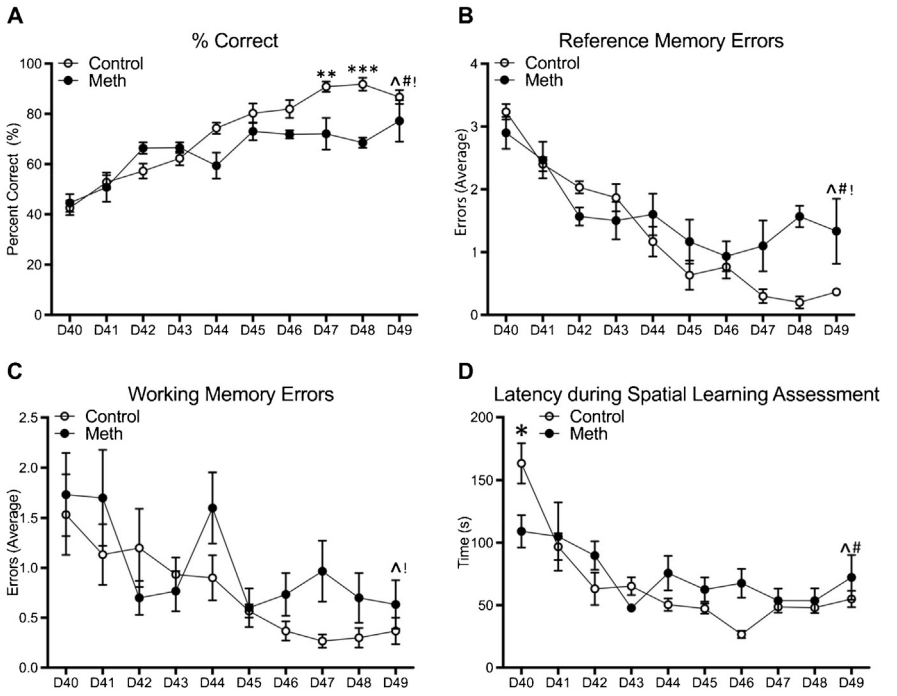

Fig. 3. VOMA impairs spatial learning. All statistical analyses involved two-way ANOVA across 10 consecutive training days (experiment days 40–49 shown on graphs) and treatment conditions. Differences between treatment conditions during asymptotic performance (training days 6–10, experiment days 45–49) were analyzed separately. (A) % Correct shows a significant effect of training days (^ $p < 0.0001$) and treatment conditions (# $p < 0.0001$). Bonferroni-corrected post hoc analyses revealed significant differences between treatment conditions on training days 8 and 9, (experiment days 47–48) (** $p < 0.01$; *** $p < 0.001$). During asymptotic performance (training days 6–10) there is a significant treatment effect (! $p < 0.05$). (B) Reference memory errors show a significant effect on training days (^ $p < 0.01$), a significant interaction (# $p < 0.01$), and a significant treatment effect during asymptotic performance (training days 6–10, ! $p < 0.01$). (C) Working memory errors show a significant effect of training days (^ $p < 0.01$), without a significant difference between treatment conditions except during asymptotic performance (training days 6–10, ! $p < .05$). (D) Latency to complete the trials show a significant effect of training days (^ $p < 0.01$), and a significant interaction between treatment conditions (# $p < 0.01$). Bonferroni post-hoc tests show a significant difference between treatment conditions on training day 1 ($p<0.05$).

$p < 0.05$; $\eta^2_G = 0.20$] for working memory errors. Together the data in Fig. 3A-C demonstrate that MA is significantly impairing the level of peak performance across multiple analyses on this spatial learning task. Analysis of latency to complete the training trials shows a significant interaction effect of treatment on training days [$F_{(9,72)} = 4.92$, $p < 0.01$; $\eta^2_G = 0.23$] and an overall significant decrease over training days [$F_{(9,72)} = 22.01$, $p < 0.01$; $\eta^2_G = 0.57$]. Post-hoc tests show a significant difference between treatment conditions on training day 1 (Bonferroni corrected t-test = 3.31, $p < 0.05$; $g = 1.89$).

http://dx.doi.org/10.1016/j.heliyon.2018.e00509

3.3. Hippocampal dopaminergic marker expression

Western blot analyses for dopaminergic markers showed a significant decrease in cytosolic TH ($t_7 = 2.67$, $p < 0.05$, $g = 1.59$; Fig. 4A). In the synaptic fraction, there was a significant increase in D1R expression ($t_8 = 3.16$, $p < 0.01$, $g = 1.81$, Fig. 4B) and a decrease in synaptic DAT expression ($t_7 = 2.16$, $p < 0.05$, $g = 1.29$, Fig. 4C).

3.4. Hippocampal inflammatory marker expression

Inflammatory markers showed a significant increase of synaptic COX-2 ($t_8 = 1.93$, $p < 0.05$, $g = 1.09$, Fig. 5A) and cytosolic COX-2 ($t_7 = 2.03$, $p < 0.05$, $g = 1.211$, Fig. 5B). Cytosolic GFAP was also significantly elevated compared to controls ($t_7 = 3.86$, $p < 0.01$, $g = -2.30$, Fig. 5C). GFAP and COX-2 increases suggest an increase in proinflammatory activity in the hippocampus. MA-induced excitotoxicity can mediate increases of GFAP to allow for astrocyte activation in response to MA-induced damage (McConnell et al., 2015). COX-2 is an inducible inflammatory activator that can signal other pathways, including prostaglandin synthesis, which can be protective or toxic to neurons (Figueiredo-Pereira et al., 2015). Fig. 5D-F shows analyses of PGE2, D2 and J2 in picograms per milligram of wet weight of tissue, indicating that PGD2 levels in control mice are at least 10-fold higher than PGE2 and PGJ2. Both PGE2 and PGD2 significantly decrease (33% and 40% respectively) with VOMA compared to controls ($t_8 = 3.95$, $p < 0.05$; $g = 2.26$, Fig. 5D. $t_8 = 3.73$, $p < 0.01$; $g = 2.13$, Fig. 5E.). PGJ2, which is a PGD2 metabolite, did not change significantly between treatment conditions (Fig. 5F).

3.5. Hippocampal synaptic plasticity marker expression

Compared to controls, VOMA produced a significant decline in glutamatergic and synaptic plasticity markers including synaptic GluA2 ($t_6 = 8.53$, $p < 0.01$, $g =$

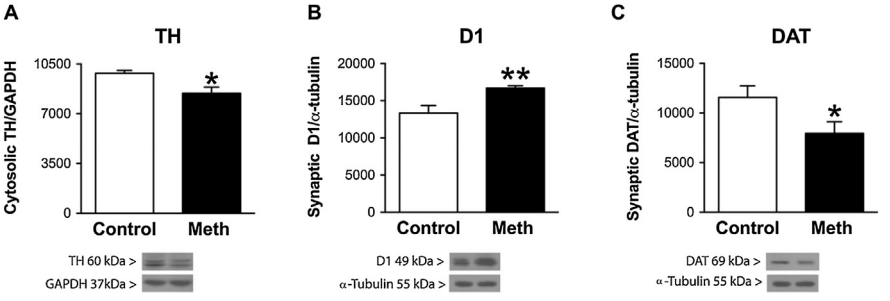

Fig. 4. Chronic VOMA affects dopaminergic marker expression. Compared to controls, VOMA decreases cytosolic TH (*$p < 0.05$; A). In the synaptic fraction, D1R significantly increased (**$p < 0.01$; B) and DAT significantly decreased (*$p < 0.05$; C) compared to controls. Representative blots show control (left band) and Meth (right band) treatments. See supplementary figures for original images of blots.

http://dx.doi.org/10.1016/j.heliyon.2018.e00509

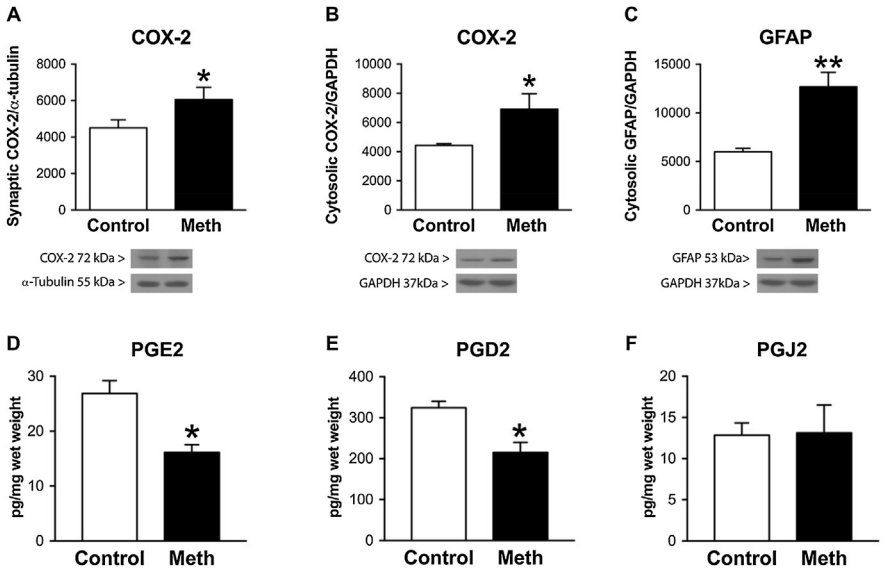

Fig. 5. Chronic VOMA increases neuroinflammation marker expression. In the synaptic (A) and cytosolic (B) fractions COX-2 levels significantly increased compared to controls ($^{*}p < 0.05$). (C) Cytosolic GFAP increased compared to controls (**$p < 0.01$). See supplementary figures for original images of blots. (D,E). PGE2 and PGD2 significantly decreased with VOMA compared to controls (*$p < 0.05$; picograms/milligram). (F). PGJ2 expression did not change significantly between treatment conditions. Representative blots show control (left band) and Meth (right band) treatments.

5.24, Fig. 6A), synaptic PSD-95 ($t_8 = 3.38$, $p < 0.01$, $g = 1.93$, Fig. 6B) and cytosolic PKMζ ($t_8 = 2.55$, *$p < 0.05$, $g = 1.46$, Fig. 6C). Cytosolic PKCι/λ expression was not altered by VOMA treatment (Fig. 6D).

4. Discussion

4.1. VOMA as a model for studying MA addiction

VOMA is a new model for assessing both the chronic and acute effects of MA. MA mixed in a palatable sweetened oatmeal mash provides a paradigm that does not require surgery or conditioning. This model permits the animal unrestricted movement that allows the experimenter to test various behavioral learning paradigms. Our results demonstrate that chronic voluntary consumption of MA results in significant spatial learning and memory deficits together with significant changes in markers reflective of MA neurotoxicity. One of the main challenges in MA research is designing an experiment that models aspects of human MA addiction. We find that this VOMA model is useful for characterizing aspects of addiction, as mice are able to titer the amount of drug administered, as reflected by a consistent level of MA consumed over several weeks. Our results indicate that the C57BL/6 mice will voluntary consume about 1.743 mg/kg bw/hr during a 3 hr MA administration period. These data suggest that if 5 mg/kg bw MA was delivered as a bolus dose to a mouse of this strain, even such a seemingly low dose

http://dx.doi.org/10.1016/j.heliyon.2018.e00509

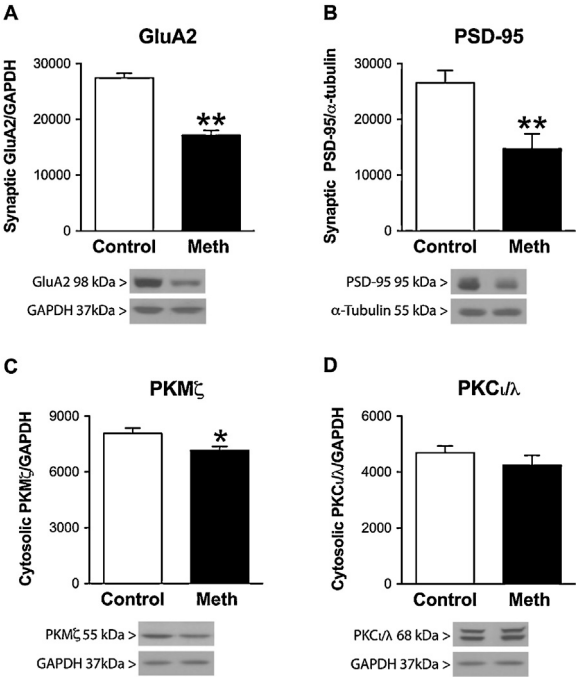

Fig. 6. Chronic VOMA decreases memory associated marker expression. In the synaptic fraction, VOMA decreased (A) GluA2 ($^{**}p < 0.01$) and (B) PSD-95 compared to controls ($^{**}p < 0.01$). (C) In the cytosolic fraction, VOMA decreased PKMζ compared to controls ($^{*}p < 0.05$). (D) VOMA did not significantly affect cytosolic PKCι/λ expression. Representative blots show control (left band) and Meth (right band) treatments. See supplementary figures for original images of blots.

is considerably higher than would be consumed voluntarily. Whether there is a difference between an injection of 5 mg/kg bw compared to voluntarily consuming this amount over a 3 hr period remains to be determined. Other MA models have used appetitive paradigms (Keith et al., 2013) or drinking paradigms (Olsen et al., 2013) that also demonstrate the short-term behavioral and neurochemical changes associated with small doses of voluntary MA consumption. In our current study, we examine the behavioral and neurochemical effects of chronic voluntary MA as a way to more accurately model human MA addiction.

Throughout 28 days of VOMA, consumption rates increase over the first 2 weeks and stabilize during the last 2 weeks. Previous self-administration models may only reveal a trend to increase consumption due to the brief (2 weeks or less) administration window. It is unclear how other self-administration models would compare to VOMA across longer periods administration (4 weeks or more). Moreover, it is important to consider how oral administration via a sweetened medium might affect VOMA. Control mice in our study consumed every presentation of water-Maypo (12 baits/day over 28 days), revealing a preference for sweetened food by this mouse line. However, mice that consumed water-Maypo laced with MA consumed less than half of the baits presented to them each

http://dx.doi.org/10.1016/j.heliyon.2018.e00509

day on average (see Results). This reveals that although a sugar preference could motivate consumption of the MA-baits, mice rapidly adapt a strategy to consume only as much MA-Maypo as they prefer. Mice on VOMA could still develop a preference to MA as a result of the sweetened medium, but more work is needed to determine this. Future studies should examine how the drug's medium affects consumption rates across long periods of MA access.

The use of an oral administration design is validated by previous work indicating that the mean half-elimination life of oral MA is not significantly different from that of the intravenous route, and that peak plasma concentration is delayed via the oral route by 3 hrs in humans, compared to other routes (Cook et al., 1992; 1993). This suggests that VOMA can model the delayed effects of MA on the brain, and very adequately reveal the prolonged neurotoxic effects of the drug. Additionally, previous work has revealed that although the injection route may be preferred by a subset of highly-addicted individuals, non-injection routes make up a high percentage of MA use in the United States (Novak and Kral, 2011). Nonetheless, our study models oral MA administration, a route not likely preferred by MA-addicted humans. Non-injection MA administration might be preferred by individuals who have not yet developed an addiction. In order to fully understand the distinct populations that abuse MA, more research is needed to clarify the onset and progression of this addiction in humans as it relates to administration routes. Future VOMA studies should examine the progression and relapse of MA consumption in VOMA in order to accurately characterize the addictive phenotype produced by our model.

4.2. MA-induces deficits in both spatial working and reference memory performance

Our results show that total MA consumption of 146.4 mg/kg bw/28 consecutive days result in a significant spatial working memory performance deficit. Our previous study reports working memory deficits following neurotoxic doses of MA (30 mg/kg bw delivered once per week for 2 weeks; 60 mg/kg bw total). These working memory deficits developed over a 4 week abstinence period (Braren et al., 2014). The working memory deficit observed in our current study may have developed much earlier based on the levels of MA consumed. However, reports by others suggest that lower doses of MA delivered chronically may have less harmful or delayed cognitive effects, compared to bolus or neurotoxic doses (Marshall et al., 2007; Simoes et al., 2007). The latter studies are consistent with the protective effects observed when escalating doses of MA are delivered over days that show reduced cognitive and neurochemical deficits, compared to neurotoxic effects and the resulting cognitive deficits that result from a bolus dose (Belcher et al., 2008; O'Neil et al., 2006; Riddle et al., 2002; Segal et al., 2003). Rapid deficits in working memory performance identified 24 hrs following a neurotoxic

http://dx.doi.org/10.1016/j.heliyon.2018.e00509

dose of MA were previously reported (Simoes et al., 2007). However, without repeated assessments over time, it is difficult to determine whether the working memory deficits are long lasting or are reflective of the short-interval between MA treatment and working memory testing. It is possible that shortly after MA administration, mice are low on seeking novelty, an effect that is rectified weeks after MA treatment as demonstrated in rat performance on the spontaneous alternation task (Friedman et al., 1998).

Following the working memory assessment, mice were tested for cognitive flexibility on the RAM. For this assessment, both working and reference memory errors were scored. The MA treated mice exhibited a lower asymptotic performance level for % correct scores and an increase in the number of reference and working memory errors compared to mice given control treatment. This is consistent with several other studies reporting spatial memory deficits following a short abstinence period (Camarasa et al., 2010; Heysieattalab et al., 2016; Williams et al., 2003). Others have shown that chronic use of MA can actually stave off MA-induced deficits, which can then be initiated following long-periods of abstinence. In this case, cognitive deficits were observed only following long-term abstinence (1–4 weeks) (Belcher et al., 2005; Braren et al., 2014; Marshall et al., 2007; North et al., 2013). The degree to which VOMA produces neuroprotection and/or can delay the neurotoxic effects of MA remains to be determined.

4.3. Chronic VOMA decreases TH and DAT while increasing D1R levels

Our previous studies revealed that acute neurotoxic doses of MA (2 × 30 mg/kg) followed by 6 weeks of forced abstinence produce long-lasting decreases in dopamine marker expression in the hippocampus (Braren et al., 2014). In our current study, we found that VOMA for 28d also produced significant decreases in these markers in the hippocampus. Previous work has shown that within days of injecting neurotoxic doses of MA, the striatum exhibits a comparable decrease in DA levels (Cappon et al., 2000; Fumagalli et al., 1998; Green et al., 1992; Guilarte et al., 2003; O'Callaghan and Miller, 1994; Xu et al., 2005). MA-induced reductions of TH and DAT in the striatum may indicate degeneration of DA axonal terminals (Fukumura et al., 1998; Lorez, 1981; Ricaurte et al., 1982; 1984). This explanation is supported by increased reactive astrogliosis associated with MA treatment (Bowyer et al., 1994; Fukumura et al., 1998; Zhu et al., 2005). We hypothesize that decreased DAT and TH together with an increase in astrogliosis reflects a degeneration of DA terminals within the hippocampus. Whether our VOMA paradigm produces similar effects in the striatum remains to be determined.

http://dx.doi.org/10.1016/j.heliyon.2018.e00509

VOMA also induced a significant increase in D1R expression. This receptor is known to mediate some of the MA-driven neurotoxic effects in the striatum (Surmeier et al., 1995) and PFC (Gonzalez et al., 2016). Selective D1R antagonists delivered prior to injections of binge doses of MA produce neuroprotective effects against the MA-induced decreases in DA, TH and DAT (Xu et al., 2005). Moreover, increases in MA-induced extracellular DA causes acute increases in striatal glutamate as a result of D1R mediated disinhibition of corticostriatal glutamate release (Mark et al., 2004). Together these findings suggest that increased D1R expression is detrimental and/or exacerbates the neurotoxic damage from MA. In contrast, it has been suggested that D1R activation is a neuroprotective response. Dopamine suppresses glutamatergic hippocampal and entorhinal neurotransmission by activation of the D1R (Behr et al., 2000). Additionally, D1R activation can reduce NMDA receptor mediated Ca^{2+} currents in hippocampal neurons, thus decreasing excitotoxicity (Lee et al., 2002). The D1R also plays a role in reducing calcium currents in striatal neurons (Surmeier et al., 1995), and in producing inhibition on N-type voltage-gated calcium channels (Kisilevsky et al., 2008). Therefore, it is possible that alterations in other receptor levels dictate whether increased D1R-levels are beneficial or detrimental. Future studies will evaluate the changes in NMDA and mGluA receptor subunits, which could add to understanding the consequences of these neurochemical changes. For example, antagonism of NMDA, AMPA or metabotropic (mGluR5) receptors can block MA-induced toxicity in the striatum (Battaglia et al., 2002; Golembiowska et al., 2003; Marshall et al., 1993) or hippocampus (Farfel et al., 1992).

4.4. Neuroinflammatory marker levels increase in the hippocampus following chronic VOMA

We show that compared to controls, GFAP and COX-2 protein levels are elevated in the hippocampus after 28d of VOMA. We propose that these changes in inflammatory markers reflect a neurodegenerative response to MA. COX catalyzes the conversion of arachidonic acid to prostaglandins (PG) and thromboxanes. COX-1 is constitutively expressed, whereas COX-2 is induced upon stimulation by various proinflammatory agents (endotoxins, cytotoxins) (Figueiredo-Pereira et al., 2015; Smith et al., 2000). Elevated levels of COX-2 in the hippocampus increase the extracellular concentration of glutamate, exacerbating glutamate-associated excitotoxicity (Anneken et al., 2013; Bezzi et al., 1998; Kelley et al., 1999; Sang et al., 2011). Our results are consistent with what is observed following neurotoxic doses of MA (Tsuji et al., 2009). Conversely, COX-2 KO mice are resistant to MA-dependent dopamine depletion in the striatum that results from high doses (Thomas and Kuhn, 2005), suggesting that COX-2 up-regulation exacerbates the neurotoxic effects of MA (Northrop and Yamamoto, 2013; Zhang et al., 2007). Other reports show temporary GFAP increases in the hippocampus 24 h after

http://dx.doi.org/10.1016/j.heliyon.2018.e00509

neurotoxic doses of MA, which return to basal levels by 7d post injection (Goncalves et al., 2010; Tsuji et al., 2009). These data suggest that the rapid increases in GFAP induced by a neurotoxic dose of MA may reflect activation of a neuroregenerative response, as this marker is expressed during neurogenesis in the subgranular zone of the dentate gyrus (Zhu and Dahlström, 2007). Based on these findings, it is possible that the accumulating (low doses) of MA during VOMA prolong the short-term increase in GFAP that has been observed following neurotoxic doses. Future studies should characterize the time course for the onset and progression of GFAP expression in the hippocampus after VOMA.

Following a regimen of neurotoxic MA administration (4 × 10 mg/kg, 2 h apart, i.p.), mice exhibit cytotoxic brain edema driven by increases in hippocampal and striatal aquaporin-4 channels on astrocytes (Leitão et al., 2017). Increased GFAP expression in the hippocampus following VOMA suggests that after chronic MA abuse, the hippocampus is vulnerable to breakdown of the blood-brain barrier resulting in cytotoxic edema. Astrocytes are one part of the complex neurovascular niche and aquaporins play a pivotal role in regulating water and cerebro-spinal fluid (CSF) flow into and out of the neuronal space (Amiry-Moghaddam et al., 2004; Jessen et al., 2015). It is unclear how and when this dysregulation in aquaporin-mediated shifts in water/CSF emerges and is resolved after chronic MA abuse. Future studies should examine the role that aquaporin-mediated cytotoxic edema plays in VOMA-induced neural and cognitive deficits.

PGE2 and PGD2 levels decrease following VOMA. PGD2 is the most abundant of the PGs in the brain followed by PGE2, and both PGs induce secretion of nerve growth factor and brain-derived neurotropic factor (Toyomoto et al., 2004). In addition, both PGD2 and PGE2 were found to have neuroprotective effects in the CNS (Masuda et al., 1986; McCullough et al., 2004; Taniguchi et al., 2007). These studies suggest that decreased levels of PGD2 and PGE2, together with increased expression of COX-2 could mediate a neurotoxic response to VOMA. It is possible that the decrease in PGE2 reflects an increase in the 15-hydroxyprostaglandin dehydrogenase (15-PGDH), a key enzyme in the metabolism of PGE2. An ALS mouse model shows that 15-PGDH increases throughout the progression of the disease specifically in GFAP positive astrocytes, while PGE2 only increased at the end stage of the disease (Miyagishi et al., 2017). No other studies have measured PGs in the hippocampus following MA. One study examined binge doses of MA on PGE2 in the striatum showing no changes in PGE2 levels up to 48 hrs following MA (Thomas and Kuhn, 2005). Further work is needed to delineate how these different MA models affect PGs across various brain regions.

PGJ2 is a product of spontaneous dehydration of PGD2, which is the most abundant prostaglandin in the brain (Hertting and Seregi, 1989) and the one that changes the most under pathological conditions (Liang et al., 2005). PGJ2 is a

http://dx.doi.org/10.1016/j.heliyon.2018.e00509

highly neurotoxic prostaglandin (Li et al., 2004b), as it impairs both the ubiquitin-proteasome pathway (Ogburn and Figueiredo-Pereira, 2006; Wang et al., 2006) and mitochondrial function (Kondo et al., 2002). This PG also up-regulates COX-2 (Li et al., 2004a), most likely leading to a positive feedback loop between itself and COX-2 (Figueiredo-Pereira et al., 2015). In supplementary studies, we have observed that PGJ2 levels increase following 6 weeks of abstinence after acute neurotoxic doses of MA (2 × 30 mg/kg; supplementary Fig. 1) and also increases following 4 weeks of abstinence after a 2 week VOMA period (25 mg/kg total MA consumed over 14d; supplementary Fig. 2). However, mice given 28d of VOMA did not exhibit increases in PGJ2 (Fig. 5F). These data suggest that abstinence may be playing a role in the increased expression of PGJ2. This finding is consistent with previous studies indicating that abstinence from MA can exacerbate memory deficits (Braren et al., 2014; North et al., 2013).

Our results suggest that the duration of abstinence and of MA-administration could play opposing roles in promoting or suppressing PGJ2 levels in the hippocampus. We hypothesize that a long period of abstinence from MA promotes PGJ2 expression, but that a longer period of MA administration mitigates it through increased dopamine release. This hypothesis is consistent with the understanding that dopamine is anti-inflammatory by inhibiting the activation of NOD-like receptor containing Pyrin domain-3 (NLRP3) inflammasome by D1R activation (Yan et al., 2015). Additional studies have shown that low doses of MA, which increase dopamine release, are neuroprotective following oxygen-glucose deprivation (Rau et al., 2016). However, it remains to be determined how abstinence from MA contributes to increases in PGJ2.

4.5. MA decreases synaptic memory markers

Our results show that the levels of PKMζ and AMPA receptor subunit GluA2 decrease following VOMA. PKMζ is important for both late-phase LTP (Serrano et al., 2005) and long-term memory maintenance across various learning paradigms (Hsieh et al., 2016; Pastalkova et al., 2006; Sacktor, 2011; Serrano et al., 2008). It is also important to note that increased GluA2 synaptic expression is important for spatial memory (Migues et al., 2010; Sebastian et al., 2013c), as is the trafficking of AMPA receptors by PKMζ (Ling et al., 2002; Yao et al., 2008). These studies are consistent with the decline in PKMζ and GluA2 levels following VOMA. We also assessed the protein levels of PKCι/λ, another atypical kinase known to support spatial memory in the conditional-PKMζ KO mouse (Tsokas et al., 2016), suggesting that PKCι/λ is active when PKMζ is compromised. PKCι/λ expression was not significantly altered following VOMA, suggesting that deficits in PKMζ may not reflect neurotoxic damage, but rather reflect poor learning.

http://dx.doi.org/10.1016/j.heliyon.2018.e00509

GluA2 is one of the four AMPA receptor subunits impermeable to Ca^{2+} and is the dominant heteromeric conformation (Geiger et al., 1995; Suzuki et al., 2003). Reduced GluA2 levels were shown to increase neurotoxicity in amyotrophic lateral sclerosis motor neurons (Lai et al., 2006; Van Damme et al., 2005). We hypothesize that decreased GluA2 mediates the spatial learning impairment as well as the elevated neurotoxic effects of MA. This is consistent with chronic MA treatment. In contrast, studies by others examining acute doses of neurotoxic MA report increased levels of GluA2 shortly after treatment (Simoes et al., 2007), suggesting that elevated hippocampal GluA2 levels may be contributing to a neuroprotective response by MA. However, after several weeks of abstinence, hippocampal GluA2 levels return to baseline (Braren et al., 2014). Together these results suggest that early after MA, hippocampal GluA2 increases as a neuroprotective mechanism, while following chronic MA a decline in hippocampal GluA2 could exacerbate MA neurotoxicity. These results are also consistent with our behavioral data, indicating that GluA2 decline in the hippocampus could underlie the spatial memory deficits found in VOMA mice.

Our results also show a significant decrease in PSD-95 protein levels. PSD-95 is primarily located in the neuronal spine head and its density reflects synaptic efficacy (Harris and Stevens, 1989). Moreover, increases in PSD-95 spine density are associated with improved memory performance (Leuner et al., 2003; Marrone, 2007; Moser et al., 1994). These findings are consistent with the poor memory performance and reduced hippocampal PSD-95 level in the MA treated mice. PSD-95 levels also increase in the forebrain following MA-induced place preference (Shibasaki et al., 2011), suggesting PSD-95 involvement in memory rather than a secondary effect of MA-induced toxicity.

5. Conclusions

Our data demonstrate that chronic VOMA leads to significant deficits in spatial learning and short-term working memory, which is consistent with reports by others. Additionally, our results show that low doses of MA consumed over a 3 hr period can produce significant neurotoxic changes in the hippocampus, reproducing the neurochemical effects observed in studies using bolus or neurotoxic doses of MA. Chronic VOMA also leads to significant decreases in TH and DAT and an increase in D1R expression as seen with neurotoxic and binge doses of MA. These neurochemical changes are accompanied by increases in both COX-2 and GFAP that were previously reported. In concert with the decline in PGE2 and PGD2 levels, these data may reflect extensive neurotoxic damage attributed to MA. Finally, decreases in synaptic markers relevant to spatial long-term memory involving both GluA2 and PKMζ are consistent with neurotoxicity-induced deficits in working memory and spatial learning. The time course for the onset and progression of these various neurochemical changes in the VOMA model remains

http://dx.doi.org/10.1016/j.heliyon.2018.e00509

to be determined. These data are consistent with what is observed in MA addicts showing low levels of dopamine, DAT and TH associated with cognitive impairment (Obermeit et al., 2013; Volkow et al., 2015). Together these studies support the significance of this VOMA mouse model in identifying risk factors and exploring potential remediation therapies against MA addiction.

Declarations

Author contribution statement

Jorge A. Avila: Conceived and designed the experiments; Performed the experiments; Analyzed and interpreted the data; Wrote the paper.

Roseanna Zanca, Denis Shor, Nicholas Paleologos: Performed the experiments.

Amber A. Alliger: Analyzed and interpreted the data.

Maria Figueiredo-Pereira, Peter A. Serrano: Conceived and designed the experiments; Wrote the paper.

Funding statement

This work was supported in part by the RCMI grant number RR003037 from the National Center for Research Resources (NCRR) to Hunter College; NIH Training Grant RISE 5R25GM060665-16 to Jorge A. Avila; and NIH 5R24DA012136-13 to Peter A. Serrano.

Competing interest statement

The authors declare no conflict of interest.

Additional information

Data associated with this study are not publicly available due to the novelty of the model and methods but is available from the corresponding author on reasonable request.

Supplementary content related to this article has been published online at http://dx.doi.org/10.1016/j.heliyon.2018.e00509.

Acknowledgements

We would like to thank Dennis Koop and his lab for their help in measuring prostaglandin levels.

References

Amiry-Moghaddam, M., Frydenlund, D., Ottersen, O., 2004. Anchoring of aquaporin-4 in brain: molecular mechanisms and implications for the physiology and pathophysiology of water transport. Neuroscience 129 (4), 997–1008.

Anneken, J.H., Cunningham, J.I., Collins, S.A., Yamamoto, B.K., Gudelsky, G.A., 2013. MDMA increases glutamate release and reduces parvalbumin-positive GABAergic cells in the dorsal hippocampus of the rat: role of cyclooxygenase. J. Neuroimmune Pharmacol. 8 (1), 58–65.

Battaglia, G., Fornai, F., Busceti, C.L., Aloisi, G., Cerrito, F., De Blasi, A., Melchiorri, D., Nicoletti, F., 2002. Selective blockade of mGlu5 metabotropic glutamate receptors is protective against methamphetamine neurotoxicity. J. Neurosci. 22 (6), 2135–2141. https://www.ncbi.nlm.nih.gov/pubmed/11896153.

Behr, J., Gloveli, T., Schmitz, D., Heinemann, U., 2000. Dopamine depresses excitatory synaptic transmission onto rat subicular neurons via presynaptic D1-like dopamine receptors. J. Neurophysiol. 84 (1), 112–119. https://www.ncbi.nlm.nih.gov/pubmed/10899189.

Belcher, A.M., Feinstein, E.M., O'Dell, S.J., Marshall, J.F., 2008. Methamphetamine influences on recognition memory: comparison of escalating and single-day dosing regimens. Neuropsychopharmacology 33 (6), 1453–1463.

Belcher, A.M., O'Dell, S.J., Marshall, J.F., 2005. Impaired object recognition memory following methamphetamine, but not p-chloroamphetamine- or d-amphetamine-induced neurotoxicity. Neuropsychopharmacology 30 (11), 2026–2034.

Bezzi, P., Carmignoto, G., Pasti, L., Vesce, S., Rossi, D., Rizzini, B.L., Pozzan, T., Volterra, A., 1998. Prostaglandins stimulate calcium-dependent glutamate release in astrocytes. Nature 391 (6664), 281–285.

Bowers, M.S., Chen, B.T., Bonci, A., 2010. AMPA receptor synaptic plasticity induced by psychostimulants: the past, present, and therapeutic future. Neuron 67 (1), 11–24.

Bowyer, J.F., Davies, D.L., Schmued, L., Broening, H.W., Newport, G.D., Slikker Jr., W., Holson, R.R., 1994. Further studies of the role of hyperthermia in methamphetamine neurotoxicity. J. Pharmacol. Exp. Ther. 268 (3), 1571–1580. https://www.ncbi.nlm.nih.gov/pubmed/8138969.

Braren, S.H., Drapala, D., Tulloch, I.K., Serrano, P.A., 2014. Methamphetamine-induced short-term increase and long-term decrease in spatial working memory affects protein Kinase M zeta (PKM(ζ), dopamine, and glutamate receptors. Front. Behav. Neurosci. 8, 438.

Cadet, J.L., Krasnova, I.N., 2009. Molecular bases of methamphetamine-induced neurodegeneration. Int. Rev. Neurobiol. 88, 101–119.

Camarasa, J., Rodrigo, T., Pubill, D., Escubedo, E., 2010. Memantine is a useful drug to prevent the spatial and non-spatial memory deficits induced by methamphetamine in rats. Pharmacol. Res. 62 (5), 450–456.

Cappon, G.D., Pu, C., Vorhees, C.V., 2000. Time-course of methamphetamine-induced neurotoxicity in rat caudate-putamen after single-dose treatment. Brain Res. 863 (1-2), 106–111. https://www.ncbi.nlm.nih.gov/pubmed/10773198.

Cook, C.E., Jeffcoat, A., Hill, J., Pugh, D., Patetta, P., Sadler, B., White, W.R., Perez-Reyes, M., 1993. Pharmacokinetics of methamphetamine self-administered to human subjects by smoking S-(+)-methamphetamine hydrochloride. Drug Metab. Dispos. 21, 717–723. https://www.ncbi.nlm.nih.gov/pubmed/8104133.

Cook, C.E., Jeffcoat, A.R., Sadler, B.M., Hill, J.M., Voyksner, R.D., Pugh, D.E., White, W.R., Perez-Reyes, M., 1992. Pharmacokinetics of oral methamphetamine and effects of repeated daily dosing in humans. Drug Metab. Dispos. 20 (6), 856–862. https://www.ncbi.nlm.nih.gov/pubmed/1362938.

Farfel, G.M., Vosmer, G.L., Seiden, L.S., 1992. The N-methyl-D-aspartate antagonist MK-801 protects against serotonin depletions induced by methamphetamine, 3, 4-methylenedioxymethamphetamine and p-chloroamphetamine. Brain Res. 595 (1), 121–127. https://www.ncbi.nlm.nih.gov/pubmed/1361410.

Figueiredo-Pereira, M.E., Rockwell, P., Schmidt-Glenewinkel, T., Serrano, P., 2015. Neuroinflammation and J2 prostaglandins: linking impairment of the ubiquitin-proteasome pathway and mitochondria to neurodegeneration. Front Mol. Neurosci. 7, 104.

Friedman, S.D., Castaneda, E., Hodge, G.K., 1998. Long-term monoamine depletion, differential recovery, and subtle behavioral impairment following methamphetamine-induced neurotoxicity. Pharmacol. Biochem. Behav. 61 (1), 35–44. https://www.ncbi.nlm.nih.gov/pubmed/9715805.

Fukumura, M., Cappon, G.D., Pu, C., Broening, H.W., Vorhees, C.V., 1998. A single dose model of methamphetamine-induced neurotoxicity in rats: effects on neostriatal monoamines and glial fibrillary acidic protein. Brain Res. 806 (1), 1–7. https://www.ncbi.nlm.nih.gov/pubmed/9739098.

Fumagalli, F., Gainetdinov, R.R., Valenzano, K.J., Caron, M.G., 1998. Role of dopamine transporter in methamphetamine-induced neurotoxicity: evidence from mice lacking the transporter. J. Neurosci. 18 (13), 4861–4869. https://www.ncbi.nlm.nih.gov/pubmed/9634552.

Geiger, J.R., Melcher, T., Koh, D.S., Sakmann, B., Seeburg, P.H., Jonas, P., Monyer, H., 1995. Relative abundance of subunit mRNAs determines gating and Ca2+ permeability of AMPA receptors in principal neurons and interneurons in rat CNS. Neuron 15 (1), 193–204. https://www.ncbi.nlm.nih.gov/pubmed/7619522.

Golembiowska, K., Konieczny, J., Wolfarth, S., Ossowska, K., 2003. Neuroprotective action of MPEP, a selective mGluR5 antagonist, in methamphetamine-induced dopaminergic neurotoxicity is associated with a decrease in dopamine outflow and inhibition of hyperthermia in rats. Neuropharmacology 45 (4), 484–492. https://www.ncbi.nlm.nih.gov/pubmed/12907309.

Goncalves, J., Baptista, S., Martins, T., Milhazes, N., Borges, F., Ribeiro, C.F., Malva, J.O., Silva, A.P., 2010. Methamphetamine-induced neuroinflammation and neuronal dysfunction in the mice hippocampus: preventive effect of indomethacin. Eur. J. Neurosci. 31 (2), 315–326.

Gonzalez, B., Rivero-Echeto, C., Muniz, J.A., Cadet, J.L., Garcia-Rill, E., Urbano, F.J., Bisagno, V., 2016. Methamphetamine blunts Ca(2 +) currents and excitatory synaptic transmission through D1/5 receptor-mediated mechanisms in the mouse medial prefrontal cortex. Addict. Biol. 21 (3), 589–602.

Green, A.R., De Souza, R.J., Williams, J.L., Murray, T.K., Cross, A.J., 1992. The neurotoxic effects of methamphetamine on 5-hydroxytryptamine and dopamine in brain: evidence for the protective effect of chlormethiazole. Neuropharmacology 31 (4), 315–321. https://www.ncbi.nlm.nih.gov/pubmed/1381816.

Guilarte, T.R., Nihei, M.K., McGlothan, J.L., Howard, A.S., 2003. Methamphetamine-induced deficits of brain monoaminergic neuronal markers: distal axotomy or neuronal plasticity. Neuroscience 122 (2), 499–513. https://www.ncbi.nlm.nih.gov/pubmed/14614914.

Harris, K.M., Stevens, J.K., 1989. Dendritic spines of CA 1 pyramidal cells in the rat hippocampus: serial electron microscopy with reference to their biophysical characteristics. J. Neurosci. 9 (8), 2982–2997. https://www.ncbi.nlm.nih.gov/pubmed/2769375.

Hertting, G., Seregi, A., 1989. Formation and function of eicosanoids in the central nervous system. Ann. NY Acad. Sci. 559, 84–99. https://www.ncbi.nlm.nih.gov/pubmed/2672946.

Heysieattalab, S., Naghdi, N., Zarrindast, M.R., Haghparast, A., Mehr, S.E., Khoshbouei, H., 2016. The effects of GABAA and NMDA receptors in the shell-accumbens on spatial memory of METH-treated rats. Pharmacol. Biochem. Behav. 142, 23–35.

 http://dx.doi.org/10.1016/j.heliyon.2018.e00509

Hsieh, C., Tsokas, P., Serrano, P., Hernandez, A.I., Tian, D., Cottrell, J.E., Shouval, H.Z., Fenton, A.A., Sacktor, T.C., 2016. Persistent increased PKMzeta in long-term and remote spatial memory. Neurobiol. Learn Mem.

Jarrard, L.E., 1978. Selective hippocampal lesions: differential effects on performance by rats of a spatial task with preoperative versus postoperative training. J. Comp. Physiol. Psychol. 92 (6), 1119–1127. https://www.ncbi.nlm.nih.gov/pubmed/755058.

Jessen, N.A., Munk, A.S.F., Lundgaard, I., Nedergaard, M., 2015. The glymphatic system: a beginner's guide. Neurochem. Res. 40 (12), 2583–2599.

Kalivas, P.W., Volkow, N.D., 2011. New medications for drug addiction hiding in glutamatergic neuroplasticity. Mol. Psychiatry 16 (10), 974–986.

Keith, D.R., Hart, C.L., Robotham, M., Tariq, M., Le Sauter, J., Silver, R., 2013. Time of day influences the voluntary intake and behavioral response to methamphetamine and food reward. Pharmacol. Biochem. Behav. 110, 117–126.

Kelley, K.A., Ho, L., Winger, D., Freire-Moar, J., Borelli, C.B., Aisen, P.S., Pasinetti, G.M., 1999. Potentiation of excitotoxicity in transgenic mice over-expressing neuronal cyclooxygenase-2. Am. J. Pathol. 155 (3), 995–1004.

Kisilevsky, A.E., Mulligan, S.J., Altier, C., Iftinca, M.C., Varela, D., Tai, C., Chen, L., Hameed, S., Hamid, J., Macvicar, B.A., Zamponi, G.W., 2008. D1 receptors physically interact with N-type calcium channels to regulate channel distribution and dendritic calcium entry. Neuron 58 (4), 557–570.

Kondo, M., Shibata, T., Kumagai, T., Osawa, T., Shibata, N., Kobayashi, M., Sasaki, S., Iwata, M., Noguchi, N., Uchida, K., 2002. 15-Deoxy-Delta(12,14)-prostaglandin J(2): the endogenous electrophile that induces neuronal apoptosis. Proc. Natl. Acad. Sci. USA 99 (11), 7367–7372.

Lai, C., Xie, C., McCormack, S.G., Chiang, H.C., Michalak, M.K., Lin, X., Chandran, J., Shim, H., Shimoji, M., Cookson, M.R., Huganir, R.L., Rothstein, J. D., Price, D.L., Wong, P.C., Martin, L.J., Zhu, J.J., Cai, H., 2006. Amyotrophic lateral sclerosis 2-deficiency leads to neuronal degeneration in amyotrophic lateral sclerosis through altered AMPA receptor trafficking. J. Neurosci. 26 (45), 11798–11806.

Lakens, D., 2013. Calculating and reporting effect sizes to facilitate cumulative science: a practical primer for t-tests and ANOVAs. Front. Psychol. 4, 863.

LaVoie, M.J., Card, J.P., Hastings, T.G., 2004. Microglial activation precedes dopamine terminal pathology in methamphetamine-induced neurotoxicity. Exp. Neurol. 187 (1), 47–57.

 http://dx.doi.org/10.1016/j.heliyon.2018.e00509

Lee, F.J., Xue, S., Pei, L., Vukusic, B., Chery, N., Wang, Y., Wang, Y.T., Niznik, H.B., Yu, X.M., Liu, F., 2002. Dual regulation of NMDA receptor functions by direct protein-protein interactions with the dopamine D1 receptor. Cell 111 (2), 219–230. https://www.ncbi.nlm.nih.gov/pubmed/12408866.

Leitão, R.A., Sereno, J., Castelhano, J.M., Gonçalves, S.I., Coelho-Santos, V., Fontes-Ribeiro, C., Castelo-Branco, M., Silva, A.P., 2017. Aquaporin-4 as a New Target against Methamphetamine-Induced Brain Alterations: Focus on the Neurogliovascular Unit and Motivational Behavior. Mol. Neurobiol., 1–14.

Leuner, B., Falduto, J., Shors, T.J., 2003. Associative memory formation increases the observation of dendritic spines in the hippocampus. J. Neurosci. 23 (2), 659–665. https://www.ncbi.nlm.nih.gov/pubmed/12533625.

Li, Z., Jansen, M., Ogburn, K., Salvatierra, L., Hunter, L., Mathew, S., Figueiredo-Pereira, M.E., 2004a. Neurotoxic prostaglandin J2 enhances cyclooxygenase-2 expression in neuronal cells through the p38MAPK pathway: a death wish? J. Neurosci. Res. 78 (6), 824–836.

Li, Z., Melandri, F., Berdo, I., Jansen, M., Hunter, L., Wright, S., Valbrun, D., Figueiredo-Pereira, M.E., 2004b. Delta12-Prostaglandin J2 inhibits the ubiquitin hydrolase UCH-L1 and elicits ubiquitin-protein aggregation without proteasome inhibition. Biochem. Biophys. Res. Commun. 319 (4), 1171–1180.

Liang, X., Wu, L., Hand, T., Andreasson, K., 2005. Prostaglandin D2 mediates neuronal protection via the DP1 receptor. J. Neurochem. 92 (3), 477–486.

Ling, D.S., Benardo, L.S., Serrano, P.A., Blace, N., Kelly, M.T., Crary, J.F., Sacktor, T.C., 2002. Protein kinase Mzeta is necessary and sufficient for LTP maintenance. Nat. Neurosci. 5 (4), 295–296.

Lorez, H., 1981. Fluorescence histochemistry indicates damage of striatal dopamine nerve terminals in rats after multiple doses of methamphetamine. Life Sci. 28 (8), 911–916. https://www.ncbi.nlm.nih.gov/pubmed/7219059.

Mark, K.A., Soghomonian, J.J., Yamamoto, B.K., 2004. High-dose methamphetamine acutely activates the striatonigral pathway to increase striatal glutamate and mediate long-term dopamine toxicity. J. Neurosci. 24 (50), 11449–11456.

Marrone, D.F., 2007. Ultrastructural plasticity associated with hippocampal-dependent learning: a meta-analysis. Neurobiol. Learn Mem. 87 (3), 361–371.

Marshall, J.F., Belcher, A.M., Feinstein, E.M., O'Dell, S.J., 2007. Methamphetamine-induced neural and cognitive changes in rodent. Addiction 102 (Suppl 1), 61–69.

 http://dx.doi.org/10.1016/j.heliyon.2018.e00509

Marshall, J.F., O'Dell, S.J., Weihmuller, F.B., 1993. Dopamine-glutamate interactions in methamphetamine-induced neurotoxicity. J. Neural. Transm. Gen. Sect. 91 (2-3), 241–254. https://www.ncbi.nlm.nih.gov/pubmed/8099799.

Masuda, Y., Ochi, Y., Ochi, Y., Karasawa, T., Hatano, N., Kadokawa, T., Shimizu, M., 1986. Protective effect of prostaglandins D2, E1 and I2 against cerebral hypoxia/anoxia in mice. Naunyn Schmiedebergs Arch. Pharmacol. 334 (3), 282–289. https://www.ncbi.nlm.nih.gov/pubmed/3543699.

McCann, U.D., Kuwabara, H., Kumar, A., Palermo, M., Abbey, R., Brasic, J., Ye, W., Alexander, M., R.F. Dannals, Wong, D.F., Ricaurte, G.A., 2008. Persistent cognitive and dopamine transporter deficits in abstinent methamphetamine users. Synapse 62 (2), 91–100.

McConnell, S.E., O'Banion, M.K., Cory-Slechta, D.A., Olschowka, J.A., Opanashuk, L.A., 2015. Characterization of binge-dosed methamphetamine-induced neurotoxicity and neuroinflammation. Neurotoxicology 50, 131–141.

McCullough, L., Wu, L., Haughey, N., Liang, X., Hand, T., Wang, Q., Breyer, R. M., Andreasson, K., 2004. Neuroprotective function of the PGE2 EP2 receptor in cerebral ischemia. J. Neurosci. 24 (1), 257–268.

Migues, P.V., Hardt, O., Wu, D.C., Gamache, K., Sacktor, T.C., Wang, Y.T., Nader, K., 2010. PKMzeta maintains memories by regulating GluR2-dependent AMPA receptor trafficking. Nat. Neurosci. 13 (5), 630–634.

Miyagishi, H., Kosuge, Y., Takano, A., Endo, M., Nango, H., Yamagata-Murayama, S., Hirose, D., Kano, R., Tanaka, Y., Ishige, K., Ito, Y., 2017. Increased Expression of 15-Hydroxyprostaglandin Dehydrogenase in Spinal Astrocytes During Disease Progression in a Model of Amyotrophic Lateral Sclerosis. Cell Mol. Neurobiol. 37 (3), 445–452.

Moser, M.B., Trommald, M., Andersen, P., 1994. An increase in dendritic spine density on hippocampal CA1 pyramidal cells following spatial learning in adult rats suggests the formation of new synapses. Proc. Natl. Acad. Sci. USA 91 (26), 12673–12675. https://www.ncbi.nlm.nih.gov/pubmed/7809099.

Narita, M., Miyatake, M., Shibasaki, M., Tsuda, M., Koizumi, S., Narita, M., Yajima, Y., Inoue, K., Suzuki, T., 2005. Long-lasting change in brain dynamics induced by methamphetamine: enhancement of protein kinase C-dependent astrocytic response and behavioral sensitization. J. Neurochem. 93 (6), 1383–1392.

NIDA, 2013. Methamphetamine. Retrieved December 13, 2016 https://www.drugabuse.gov/publications/research-reports/methamphetamine.

Nogues, X., Micheau, J., Jaffard, R., 1994. Protein kinase C activity in the hippocampus following spatial learning tasks in mice. Hippocampus 4 (1), 71–77.

 http://dx.doi.org/10.1016/j.heliyon.2018.e00509

North, A., Swant, J., Salvatore, M.F., Gamble-George, J., Prins, P., Butler, B., Mittal, M.K., Heltsley, R., Clark, J.T., Khoshbouei, H., 2013. Chronic methamphetamine exposure produces a delayed, long-lasting memory deficit. Synapse 67 (5), 245–257.

Northrop, N.A., Yamamoto, B.K., 2013. Cyclooxygenase activity contributes to the monoaminergic damage caused by serial exposure to stress and methamphetamine. Neuropharmacology 72, 96–105.

Novak, S.P., Kral, A.H., 2011. Comparing injection and non-injection routes of administration for heroin, methamphetamine, and cocaine users in the United States. J. Addict. Dis. 30 (3), 248–257.

O'Callaghan, J.P., Miller, D.B., 1994. Neurotoxicity profiles of substituted amphetamines in the C57BL/6J mouse. J. Pharmacol. Exp. Ther. 270 (2), 741–751. https://www.ncbi.nlm.nih.gov/pubmed/8071867.

O'Callaghan, J.P., Sriram, K., 2005. Glial fibrillary acidic protein and related glial proteins as biomarkers of neurotoxicity. Expert Opin. Drug Saf. 4 (3), 433–442.

O'Neil, M.L., Kuczenski, R., Segal, D.S., Cho, A.K., Lacan, G., Melega, W.P., 2006. Escalating dose pretreatment induces pharmacodynamic and not pharmacokinetic tolerance to a subsequent high-dose methamphetamine binge. Synapse 60 (6), 465–473.

Obermeit, L.C., Cattie, J.E., Bolden, K.A., Marquine, M.J., Morgan, E.E., Franklin Jr., D.R., Atkinson, J.H., Grant, I., Woods, S.P., The Translational Methamphetamine AIDS Research Center (TMARC) Group, 2013. Attention-deficit/hyperactivity disorder among chronic methamphetamine users: frequency, persistence, and adverse effects on everyday functioning. Addict. Behav. 38 (12), 2874–2878.

Ogburn, K.D., Figueiredo-Pereira, M.E., 2006. Cytoskeleton/endoplasmic reticulum collapse induced by prostaglandin J2 parallels centrosomal deposition of ubiquitinated protein aggregates. J. Biol. Chem. 281 (32), 23274–23284.

Olsen, R.H., Allen, C.N., Derkach, V.A., Phillips, T.J., Belknap, J.K., Raber, J., 2013. Impaired memory and reduced sensitivity to the circadian period lengthening effects of methamphetamine in mice selected for high methamphetamine consumption. Behav. Brain Res. 256, 197–204.

Olton, D.S., Papas, B.C., 1979. Spatial memory and hippocampal function. Neuropsychologia 17 (6), 669–682. https://www.ncbi.nlm.nih.gov/pubmed/522981.

Pastalkova, E., Serrano, P., Pinkhasova, D., Wallace, E., Fenton, A.A., Sacktor, T.C., 2006. Storage of spatial information by the maintenance mechanism of LTP. Science 313 (5790), 1141–1144.

 http://dx.doi.org/10.1016/j.heliyon.2018.e00509

Rau, T., Ziemniak, J., Poulsen, D., 2016. The neuroprotective potential of low-dose methamphetamine in preclinical models of stroke and traumatic brain injury. Prog. Neuropsychopharmacol. Biol. Psychiatry 64, 231–236.

Ricaurte, G.A., Guillery, R.W., Seiden, L.S., Schuster, C.R., Moore, R.Y., 1982. Dopamine nerve terminal degeneration produced by high doses of methylamphetamine in the rat brain. Brain Res. 235 (1), 93–103. https://www.ncbi.nlm.nih.gov/pubmed/6145488.

Ricaurte, G.A., Seiden, L.S., Schuster, C.R., 1984. Further evidence that amphetamines produce long-lasting dopamine neurochemical deficits by destroying dopamine nerve fibers. Brain Res. 303 (2), 359–364. https://www.ncbi.nlm.nih.gov/pubmed/6744029.

Riddle, E.L., Kokoshka, J.M., Wilkins, D.G., Hanson, G.R., Fleckenstein, A.E., 2002. Tolerance to the neurotoxic effects of methamphetamine in young rats. Eur. J. Pharmacol. 435 (2-3), 181–185. https://www.ncbi.nlm.nih.gov/pubmed/11821024.

Sacktor, T.C., 2011. How does PKMzeta maintain long-term memory? Nat. Rev. Neurosci. 12 (1), 9–15.

Sang, N., Yun, Y., Yao, G.Y., Li, H.Y., Guo, L., Li, G.K., 2011. SO(2)-induced neurotoxicity is mediated by cyclooxygenases-2-derived prostaglandin E(2) and its downstream signaling pathway in rat hippocampal neurons. Toxicol. Sci. 124 (2), 400–413.

Sebastian, V., Diallo, A., Ling, D.S., Serrano, P.A., 2013a. Robust training attenuates TBI-induced deficits in reference and working memory on the radial 8-arm maze. Front. Behav. Neurosci. 7, 38.

Sebastian, V., Estil, J.B., Chen, D., Schrott, L.M., Serrano, P.A., 2013b. Acute physiological stress promotes clustering of synaptic markers and alters spine morphology in the hippocampus. PLoS One 8 (10) e79077.

Sebastian, V., Vergel, T., Baig, R., Schrott, L.M., Serrano, P.A., 2013c. PKMzeta differentially utilized between sexes for remote long-term spatial memory. PLoS One 8 (11) e81121.

Segal, D.S., Kuczenski, R., O'Neil, M.L., Melega, W.P., Cho, A.K., 2003. Escalating dose methamphetamine pretreatment alters the behavioral and neurochemical profiles associated with exposure to a high-dose methamphetamine binge. Neuropsychopharmacology 28 (10), 1730–1740.

Sekine, Y., Ouchi, Y., Sugihara, G., Takei, N., Yoshikawa, E., Nakamura, K., Iwata, Y., Tsuchiya, K.J., Suda, S., Suzuki, K., Kawai, M., Takebayashi, K., Yamamoto, S., Matsuzaki, H., Ueki, T., Mori, N., Gold, M.S., Cadet, J.L., 2008.

http://dx.doi.org/10.1016/j.heliyon.2018.e00509

Methamphetamine causes microglial activation in the brains of human abusers. J. Neurosci. 28 (22), 5756–5761.

Serrano, P., Friedman, E.L., Kenney, J., Taubenfeld, S.M., Zimmerman, J.M., Hanna, J., Alberini, C., Kelley, A.E., Maren, S., Rudy, J.W., Yin, J.C., Sacktor, T. C., Fenton, A.A., 2008. PKMzeta maintains spatial, instrumental, and classically conditioned long-term memories. PLoS Biol. 6 (12), 2698–2706.

Serrano, P., Yao, Y., Sacktor, T.C., 2005. Persistent phosphorylation by protein kinase Mzeta maintains late-phase long-term potentiation. J. Neurosci. 25 (8), 1979–1984.

Shibasaki, M., Mizuno, K., Kurokawa, K., Suzuki, T., Ohkuma, S., 2011. Role of actin depolymerizing factor in the development of methamphetamine-induced place preference in mice. Eur. J. Pharmacol. 671 (1-3), 70–78.

Simoes, P.F., Silva, A.P., Pereira, F.C., Marques, E., Grade, S., Milhazes, N., Borges, F., Ribeiro, C.F., Macedo, T.R., 2007. Methamphetamine induces alterations on hippocampal NMDA and AMPA receptor subunit levels and impairs spatial working memory. Neuroscience 150 (2), 433–441.

Smith, W.L., DeWitt, D.L., Garavito, R.M., 2000. Cyclooxygenases: structural, cellular and molecular biology. Annu. Rev. Biochem. 69, 145–182.

Surmeier, D.J., Bargas, J., Hemmings Jr., H.C., Nairn, A.C., Greengard, P., 1995. Modulation of calcium currents by a D1 dopaminergic protein kinase/phosphatase cascade in rat neostriatal neurons. Neuron 14 (2), 385–397. https://www.ncbi.nlm.nih.gov/pubmed/7531987.

Suzuki, T., Tsuzuki, K., Kameyama, K., Kwak, S., 2003. Recent advances in the study of AMPA receptors. Nihon Yakurigaku Zasshi 122 (6), 515–526. https://www.ncbi.nlm.nih.gov/pubmed/14639006.

Taniguchi, H., Mohri, I., Okabe-Arahori, H., Aritake, K., Wada, K., Kanekiyo, T., Narumiya, S., Nakayama, M., Ozono, K., Urade, Y., Taniike, M., 2007. Prostaglandin D2 protects neonatal mouse brain from hypoxic ischemic injury. J. Neurosci. 27 (16), 4303–4312.

Thomas, D.M., Kuhn, D.M., 2005. Cyclooxygenase-2 is an obligatory factor in methamphetamine-induced neurotoxicity. J. Pharmacol. Exp. Ther. 313 (2), 870–876.

Thompson, P.M., Hayashi, K.M., Simon, S.L., Geaga, J.A., Hong, M.S., Sui, Y., Lee, J.Y., Toga, A.W., Ling, W., London, E.D., 2004. Structural abnormalities in the brains of human subjects who use methamphetamine. J. Neurosci. 24 (26), 6028–6036.

Toyomoto, M., Ohta, M., Okumura, K., Yano, H., Matsumoto, K., Inoue, S., Hayashi, K., Ikeda, K., 2004. Prostaglandins are powerful inducers of NGF and BDNF production in mouse astrocyte cultures. FEBS Lett. 562 (1-3), 211–215.

Tsokas, P., Hsieh, C., Yao, Y., Lesburgueres, E., Wallace, E.J.C., Tcherepanov, A., Jothianandan, D., Hartley, B.R., Pan, L., Rivard, B., Farese, R.V., Sajan, M.P., Bergold, P.J., Hernández, A.I., Cottrell, J.E., Shouval, H.Z., Fenton, A.A., Sacktor, T.C., 2016. Compensation for PKMzeta in long-term potentiation and spatial long-term memory in mutant mice. Elife, 5.

Tsuji, T., Asanuma, M., Miyazaki, I., Miyoshi, K., Ogawa, N., 2009. Reduction of nuclear peroxisome proliferator-activated receptor gamma expression in methamphetamine-induced neurotoxicity and neuroprotective effects of ibuprofen. Neurochem. Res. 34 (4), 764–774.

UN, 2008. Amphetamines and Ecstasy – 2008 ATS Assessment. . http://www.unodc.org/documents/scientific/ATS/Global-ATS-Assessment-2008-Web.pdf.

UN, 2011. Amphetamines and Ecstasy – 2011 Global ATS Assessment. . http://www.unodc.org/documents/ATS/ATS_Global_Assessment_2011.pdf.

Van Damme, P., Braeken, D., Callewaert, G., Robberecht, W., Van Den Bosch, L., 2005. GluR2 deficiency accelerates motor neuron degeneration in a mouse model of amyotrophic lateral sclerosis. J. Neuropathol. Exp. Neurol. 64 (7), 605–612. https://www.ncbi.nlm.nih.gov/pubmed/16042312.

Vierck, J.L., Bryne, K.M., Dodson, M.V., 2000. Evaluating dot and Western blots using image analysis and pixel quantification of electronic images. Methods Cell Sci. 22 (4), 313–318. https://www.ncbi.nlm.nih.gov/pubmed/11549944.

Volkow, N.D., Wang, G.J., Smith, L., Fowler, J.S., Telang, F., Logan, J., Tomasi, D., 2015. Recovery of dopamine transporters with methamphetamine detoxification is not linked to changes in dopamine release. Neuroimage 121, 20–28.

Wang, Z., Aris, V.M., Ogburn, K.D., Soteropoulos, P., Figueiredo-Pereira, M.E., 2006. Prostaglandin J2 alters pro-survival and pro-death gene expression patterns and 26 S proteasome assembly in human neuroblastoma cells. J. Biol. Chem. 281 (30), 21377–21386.

Weber, E.M., Dallaire, J.A., Gaskill, B.N., Pritchett-Corning, K.R., Garner, J.P., 2017. Aggression in group-housed laboratory mice: why can't we solve the problem? Nature 20, 1.

Williams, M.T., Morford, L.L., Wood, S.L., Wallace, T.L., Fukumura, M., Broening, H.W., Vorhees, C.V., 2003. Developmental D-methamphetamine treatment selectively induces spatial navigation impairments in reference memory in the Morris water maze while sparing working memory. Synapse 48 (3), 138–148.

Xu, W., Zhu, J.P., Angulo, J.A., 2005. Induction of striatal pre- and postsynaptic damage by methamphetamine requires the dopamine receptors. Synapse 58 (2), 110–121.

Yan, Y., Jiang, W., Liu, L., Wang, X., Ding, C., Tian, Z., Zhou, R., 2015. Dopamine controls systemic inflammation through inhibition of NLRP3 inflammasome. Cell 160 (1-2), 62–73.

Yao, Y., Kelly, M.T., Sajikumar, S., Serrano, P., Tian, D., Bergold, P.J., Frey, J.U., Sacktor, T.C., 2008. PKM zeta maintains late long-term potentiation by N-ethylmaleimide-sensitive factor/GluR2-dependent trafficking of postsynaptic AMPA receptors. J. Neurosci. 28 (31), 7820–7827.

Zhang, X., Dong, F., Mayer, G.E., Bruch, D.C., Ren, J., Culver, B., 2007. Selective inhibition of cyclooxygenase-2 exacerbates methamphetamine-induced dopamine depletion in the striatum in rats. Neuroscience 150 (4), 950–958.

Zhu, H., Dahlström, A., 2007. Glial fibrillary acidic protein-expressing cells in the neurogenic regions in normal and injured adult brains. J. Neurosci. Res. 85 (12), 2783–2792. https://www.ncbi.nlm.nih.gov/pubmed/17394257.

Zhu, J.P., Xu, W., Angulo, J.A., 2005. Disparity in the temporal appearance of methamphetamine-induced apoptosis and depletion of dopamine terminal markers in the striatum of mice. Brain Res. 1049 (2), 171–181.

http://dx.doi.org/10.1016/j.heliyon.2018.e00509